

# Effect of WC addition on the Mechanical Properties and Microstructure of CrFeCoNi High Entropy Alloy by Powder Metallurgy Technique

\*A. Hegazy Khallaf<sup>1</sup>, M. Bhlol<sup>2</sup>, O.M. Dawood<sup>2</sup>, and Omayma A. Elkady<sup>3</sup>

<sup>1</sup>Mechanical Eng. Dept., Egyptian Academy for Engineering and Advanced Technology (EAE&AT) Affiliated to Ministry of Military Production, Cairo, Egypt

<sup>2</sup>Mechanical Eng. Dept., Faculty of Engineering, University of Helwan, Helwan, Cairo, 11792

<sup>3</sup>Powder Technology Department, Central Metallurgical R&D Institute, P.O. 87, Helwan, 11421 Cairo, Egypt

## Abstract.

(CrFeCoNi) high entropy alloy (HEA) was reinforced with variety of weight percentages from 5 to 20 wt.% WC particles, and prepared by powder metallurgy. The mixed powders were compacted under 700 MPa and then the green (cold pressed) samples sintered at 1200 °C in a vacuum furnace for 90 min. Density, phase composition, and microstructure of sintered samples were investigated. Hardness, compressive strength, and wear resistance were estimated. The results revealed that the relative density was decreased. XRD revealed the formation of FCC matrix phase and new carbide phases like Cr-rich carbide and W-rich carbide phases. Scanning electron microscope (SEM) results show a good distribution of the carbide phases over the alloy matrix. Compressive strength is improved by WC addition, at the same time the ductility was decreased. The hardness of the investigated HEAs was increased gradually with the increasing of WC content about 510.71 HV up to 614.64 HV at room temperature with improvement percentage 20.35%. Also, the wear rate of 0 wt.% WC HEA is (1.70E-04) which is approximately 4.5 times higher than the wear rate of 20 wt.% WC HEA (3.81E-05), this means that wear resistance is significantly improved with the increase of WC content.

**Keywords:** High Entropy Alloy, Powder Metallurgy, Microstructure, Micro-hardness, Wear Resistance.

## 1. Introduction

Cutting tool steels are commonly used in machining, assembling, and sealing parts. Traditional cutting tool steels are featured by high hardness, high strength and good wear resistance. However, it normally has many elements and the phase structures are complicated and difficult to manage (Yilbas et al., 2014). Meanwhile, complex-shaped components are hard to manufacture due to the high hardness of cutting tool steels. Cutting tool steels, on the other hand, still need to be enhanced in terms of corrosion resistance. Cutting tool steels, for example, are inapplicable in a salty and oxidizing environment (Torralba & Venkatesh Kumarán, 2021).

High-entropy alloys were developed recent years, they have at least five principal elements with 5 – 35 at.% for each element (Tung et al., 2007). Recently HEAs caught much attentions in which they are containing four or five metallic elements in close-to-equiatomic proportions (J. Y. He et al., 2016). HEAs are usually single-phase solid solutions (Cantor et al., 2004), with outstanding properties such as high strength, ductility, and corrosion resistance (F. He et al., 2017; Poletti et al., 2017; Tang et al., 2015). These characteristics also make HEAs suitable for structural applications such as cutting tool steels.

The properties of HEAs are modified by addition of element, compound, or a second phase. Tungsten (W) has a remarkable effect on the micro-hardness and wear resistance of CoCrFeNi HEA (Shang, Axinte, Sun, et al., 2017). Ti addition affected the wear resistance of AlCoCrFeNiTi<sub>x</sub> HEA, especially the AlCoCrFeNiTi<sub>0.5</sub> HEA, which showed superior wear resistance compared to the bearing steel (Löbel et al., 2018). Furthermore, tungsten carbide (WC) is an appealing reinforcement-phase that has been used in many alloy structures (Huang et al., 2018; Zhou et al., 2018). Juan Xu et al. and C. shang et al. studied the microstructure and properties of CoCrFeNi (WC) high-entropy alloy coatings prepared by mechanical alloying and hot consolidation techniques (Shang, Axinte, Ge, et al., 2017; Xu et al., 2019).

Although the design strategy of HEAs implies that there would be hundreds of new alloy systems, current studies focus more attention on CrCoFeNi-based alloys (Hsu et al., 2010; Tsai et al., 2017), such as high wear resistance AlCo<sub>1.5</sub>CrFeNi<sub>1.5</sub>Ti system HEAs (Chuang et al., 2011), high room temperature strength AlCoCrFeNiV system HEAs (Dong et al., 2014), and high oxidation resistance AlCoCrCuFeNi system HEAs (Dąbrowa et al., 2017). Some recent research has focused on cemented carbides with HEA binder phases. The HEA binders, as possible cobalt substitutes, not only effectively restrict the development of WC grains, but also aid in the creation of WC-HEA composites with superior overall mechanical characteristics than typical WC-Co alloys (Luo et al., 2021).

In this work, CrFeCoNi HEAs are prepared using a powder metallurgy technique with the addition of 5 to 20% WC particles in order to be used as high-strength cutting tools with good machinability. The prepared HEAs' mechanical properties, microstructure, compression, hardness, and wear resistance are all investigated in detail. As a result, the aim of this research is to develop new cutting tool generations from  $(\text{CrFeCoNi})_{1-x}(\text{WC})_x$  ( $x=0-20$  wt.%) HEAs with a high wear resistance and high strength.

## 2. Experimental work

### 2.1. Materials

Alloy elements which implemented in this investigation were Cr, Fe, Co, Ni, and WC powders with high purity (more than 99.5 %). Particle size less than 70  $\mu\text{m}$  were mechanically alloyed to synthesize CrFeCoNi HEA powders.

### 2.2. Synthesis of High Entropy Alloys

The starting elemental powders are mixed and milled in a high-energy roll ball mill (Changsha Tianchuang, Powder Technology Co., Ltd.) at 180 rpm, in a dry condition under a protective argon atmosphere to prevent oxidation. High-performance stainless-steel vial (1500 cc) and balls were utilized, and the ball-to-powder ratio (BPR) was 10:1. The diameters of milling balls used were 3, 6 and 10 mm. The CrFeCoNi HEA powders were milled for 25 hr., to avoid powder overheating.

The ball milling process was applied in a cyclic mode with stop intervals 15 min each 1 h, and then the milled powders were mixed with different weight ratios of WC particles (5, 10, 15 and 20 wt.%) in PQ-N2 planetary ball mill at 350 rpm for 1 h., to verify homogenization and to eliminate powders clusters. These parameters was selected based on A. Abu-Oqail et al. and A. M. Sadoun et al. (Abu-Oqail et al., 2019; Sadoun, Mohammed, Fathy, et al., 2020).

Cylindrical specimens of each group with 8 mm diameter and 12 mm height have been synthesized by cold pressing with a universal hydraulic piston with a uniaxial pressure of 700 MPa. The green (cold pressed) specimens were then sintered at 1200 °C for 90 min with a heating rate of 3 °C/min under a flowing argon atmosphere in a horizontal tube furnace (type XINKYO), Fig. 1 shows the heating schedule for the sintering process (Elkady et al., 2015; Sadoun, Mohammed, Elsayed, et al., 2020). The heating cycle was 3 °C/min from room temperature up to 850 °C, then holding for 30 min for the liquid phase formation of cobalt liquification. The sintering process is completed by 5 °C/min cycle up to 1200 °C, then a holding time for 90 min to complete the sintering process. Cooling under controlled atmosphere is done to protect samples from any oxidation.

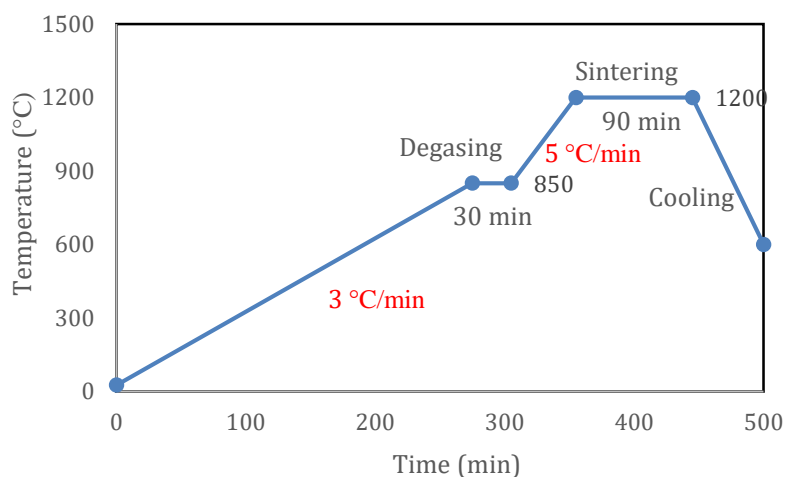


*Fig. 1 Heating schedule for the sintering process.*

### 2.3. Characterization of high entropy alloys

The density of the sintered samples were measured by using the water immersion technique (Archimedes principle) using water as a floating liquid according to the standard (ASTM B962-15) (ASTM International, 2013), and compared with the theoretical density which is calculated based on the classical law of mixtures to obtain a varying degree of densifications (Luo et al., 2018). The sintered samples were weighed at room temperature in air and in distilled water, and then the bulk density was determined. The test was performed three times to ensure the repeatability of the results.

The sintered samples were grinded using grit SiC papers with grades 600, 800, 1000, 1200, and 2000 before being polished by 6  $\mu\text{m}$  and 1  $\mu\text{m}$  alumina paste for microstructural analysis. Field emission scanning electron microscope (FE-SEM) was used to examine the microstructure of the polished samples (Inspect – model s50, TIMS, Cairo, Egypt).

The compression test was performed on the HEA samples to measure the compressive strength using (Servo-hydraulic Universal Testing Machine TTM-1200 KN). For this test, cylindrical specimens have been used with a 7.5 mm diameter, a length about 10 mm, and the ratio between the length and the diameter of the samples is about 1.2 on average. A universal hardness tester INNOVA TEST (NEMESIS 9000) was used to determine the hardness of the consolidated specimens at room temperature, on the polished surface.

Wear rate was measured according to the ASTM G133-05 standard test method for Linearly Reciprocating Ball-on-Flat Sliding Wear at room temperature (Coeffi-, 2011). An aluminium oxide ball with a 3 mm radius, which moved with an average sliding speed of 20 mm/s and the applied load is 5 N. The wear volume lose was calculated by measuring the cross-sectional area of the wear path made by the aluminium oxide ball multiplied by the length of this wear path.

### 3. Results and Discussion

The effect of WC additions on the relative density of sintered samples are shown in Fig. 2. The ratio of a sample's actual to theoretical density is known as its relative density. From the figure there are two phenomena, the first one is the values of theoretical and actual densities were increased with the increase of WC powder content, this is may be due to the high density of WC relative to the rest of elements. The second phenomenon, is the relative density was decreased with the increase of the content of WC powder, and this may be due to the non-wettability problem between the ceramic WC particles and the other four elements. In which, the surface energy between them with WC is high, therefore, some agglomerations take place by increasing WC percent, consequently the relative density is decreased (B. Liu et al., 2016). Also, the hard ceramic WC particles acts as internal barriers that hinder the complete densification, therefore, by more addition of WC the densification decreases.

Figure 3 shows the XRD patterns of the  $(CrFeCoNi)_{1-x}(WC)_x$  ( $x=0-20$  wt%) HEA samples taken on the ingot cross section contains diffraction peaks. It was noticed that the pattern of each elemental constituents was disappeared, in which no peaks were recorded for Cr, Fe, Co, or Ni individually. It seems that FCC solid solution phase and two carbide phases were appeared in the patterns as shown in the figure. Three mean peaks corresponding to FCC are observed. The highest intensity of FCC peaks, is due to the good dissolution of the four elements with each other's and good sinterability.

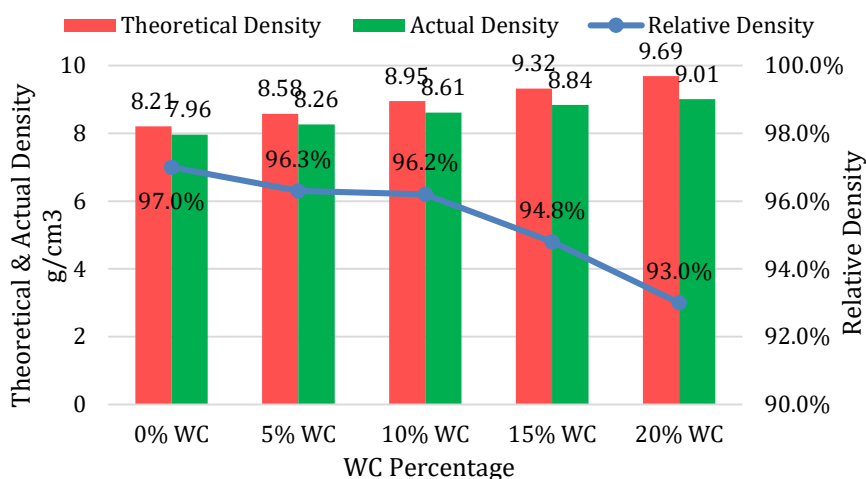


Fig. 2 Theoretical, actual, and relative densities of HEA vs. WC percentage.

The 2nd peaks are corresponding to the added WC particles. The 3rd one is belong to the formed chromium carbide phases which are  $Cr_{23}C_6$ ,  $Cr_7C_3$  and  $Cr_3C_2$  which are compatible with the previous work (Stepanov et al., 2016). The results are similar to that of the  $FeCoCrNiW_{0.3+0.5}$ .at. % C alloy, and to  $(FeCoCrNi)_{1-x}(WC)_x$  ( $x=3-11$ , at. %) (Poletti et al., 2017; Zhou et al., 2018). The increase of WC content does not affect the phase compositions of the  $(CrFeCoNi)_{1-x}(WC)_x$  HEAs, but it improves peaks intensity from W-rich and Cr-rich carbides.

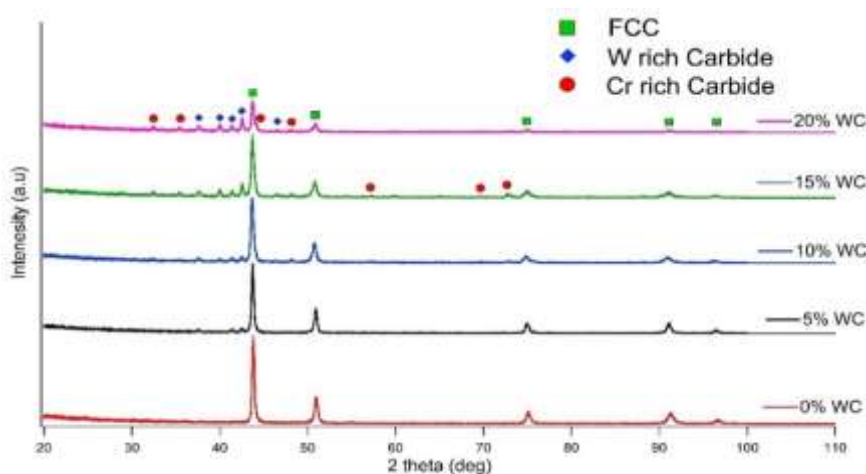
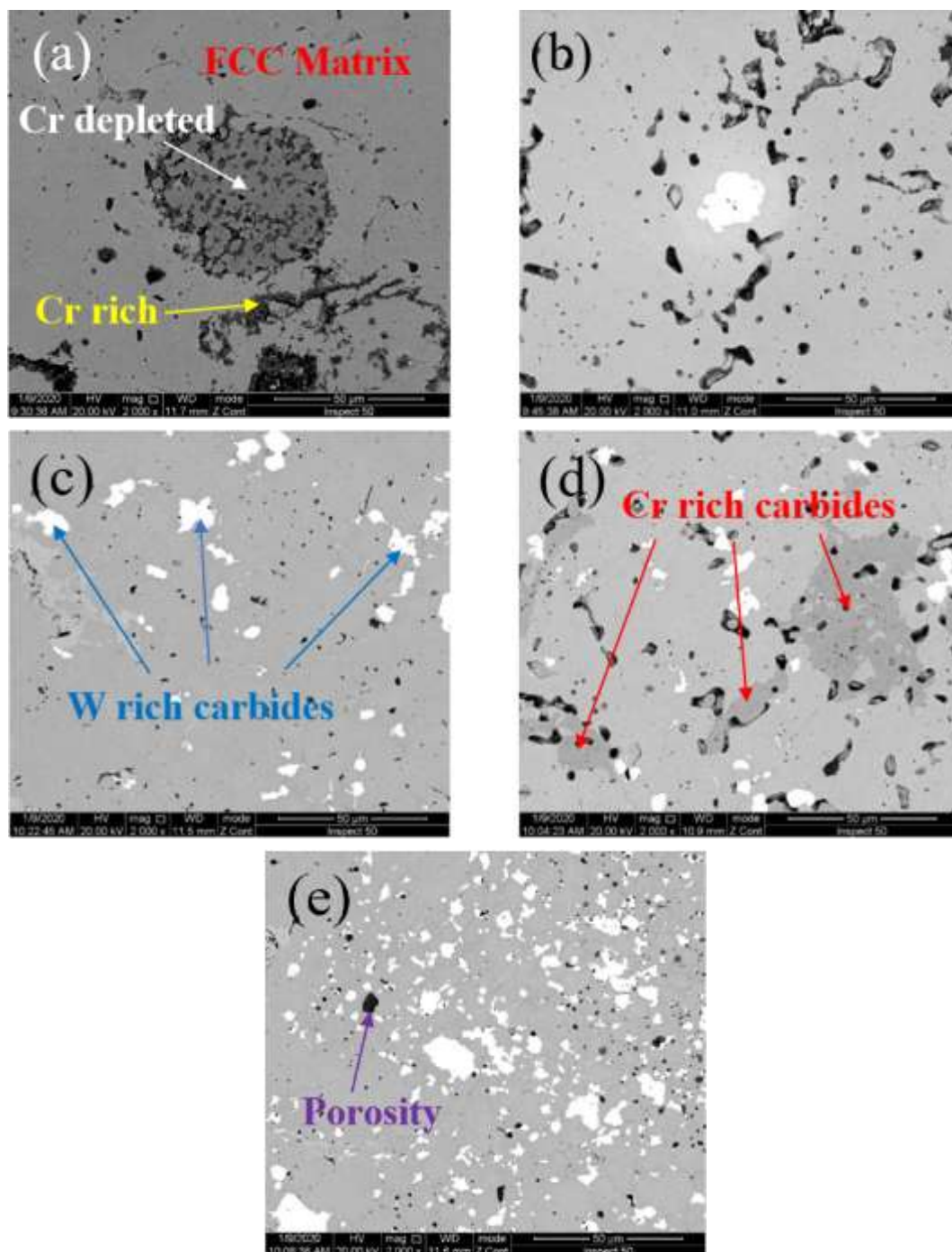


Fig. 3 XRD patterns of  $(CrFeCoNi)_{1-x}(WC)_x$  ( $x=0-20$  wt.%) HEAs.

High-temperature sintering can result in element alloying. The W-rich carbide is formed directly from the original WC particles, while the Cr-rich phases are formed by the diffusion and reaction of Cr and C (Yeh, 2013). The intensities of the WC peaks and chromium carbide ones are increased by increasing the WC percent, and no any oxides were recorded due to the controlled mixing and sintering process.

Fig. 4 shows SEM images of the  $(\text{CrFeCoNi})_{1-x}(\text{WC})_x$  ( $x=0-20$  wt.%) HEA at 2000X. In Fig. 4 (a) Cr rich phases inside the FCC matrix are appeared as dark gray areas. There are two types of Cr-rich phases, the dark gray phase in a size of sub-microns (Cr percentage exceeded 80 wt.%) which embedded in the light gray phase called Cr depleted phases (Cr percentage lower than 60 wt.%). Also, there are black areas around the Cr rich phase which presents the aggregates of the other elemental particles of the prepared HEA.

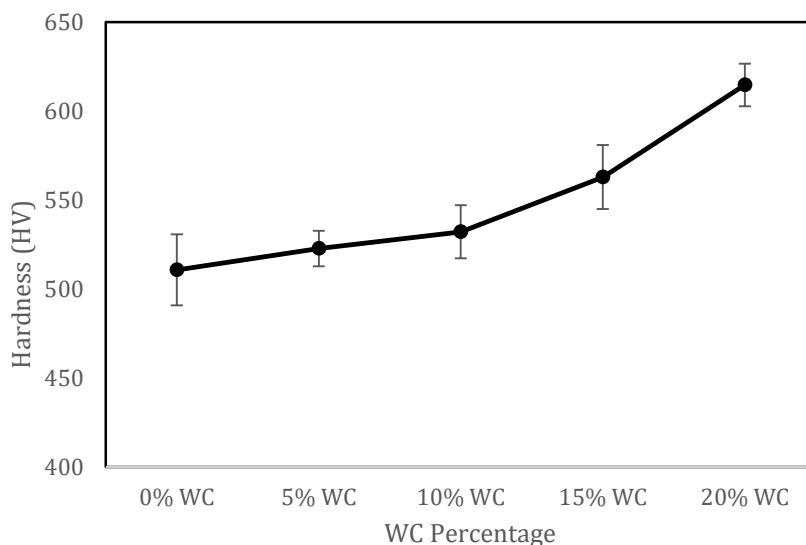


**Fig. 4 SEM Micrographs of the  $(\text{CrFeCoNi})_{1-x}(\text{WC})_x$  HEAs with a value of  $x$  equal (a)0 wt.% WC (b)5 wt.% WC (c)10 wt.% WC (d)15 wt.% WC (e)20 wt.% WC.**

Reinforcing the alloy with WC as shown in b, c, d, and e images, new phases have been appeared. There are two zones appear inside the FCC matrix, the bright phase which is the W-rich carbide phase with a particle size around 5-10 μm, and the dark gray area which is the Cr-rich carbide phase. Both of them are distributed homogenously all over the alloy matrix. Some agglomerations are observed by increasing WC percent due to the non-wettability between WC as a ceramic material and the other four metallic elements (Sadoun, Mohammed, Elsayed, et al., 2020). In which surface energy between WC and the alloy elements are large so, the contact

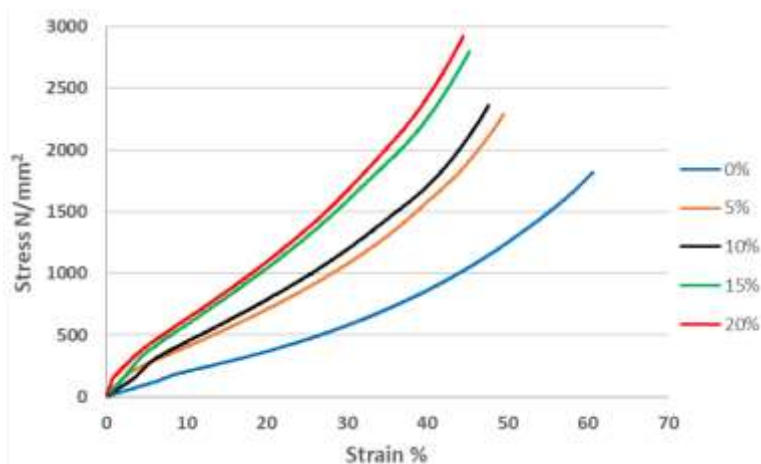
angle between them is very large, consequently agglomerations take place. It's also noticeable that some black areas appear in the microstructure due to the presence of some holes or pores, which are appear due to the relative density of the HEAs didn't reach 100% as a result of agglomerations.

Figure 5 presents the effect of WC additions on the hardness values of the alloy under test. The curve shows a gradual increase in the hardness values with WC additions. As the HEAs free from WC has about 510.71 HV value, 20 wt% WC alloy recorded 614.64 HV at room temperature. This may be attributed to the high hardness of WC particles which is 2400 HV. Therefore, incorporation of a hard ceramic material such as WC in soft elements like Cr, Co, & Ni gives a strength for the overall prepared samples. Also, WC particles acts as internal balls which makes grain refinement, so the hardness values are increased by increasing WC percent due to grain refinement, according to Hall-petch equation that states the enhancement of hardness by reduction of the particle size (Yehia et al., 2020). Also, the formed Cr-carbide phases increases the hardness.



**Fig. 5 Hardness of the  $(CrFeCoNi)_{1-x}(WC)_x$  HEAs.**

The compression strength test was used to measure the deformation behaviour of the  $(CrFeCoNi)_{1-x}(WC)_x$  ( $x=0-20$  wt.%) HEAs. Fig. 6 shows the stress – strain curves for all the samples fabricated and sintered at 1200 °C. The results showed that by increasing the WC percentage, there is an obvious enhancement of the compressive strength gradually for the HEA specimens. This may be due to the good mechanical properties, high strength, and high hardness of WC, and the good distribution of the WC particles inside the alloy helped to raise the compressive strength with the increase of WC percentage. Also, the formation of chromium carbide phase, as detected from the XRD results. At the same time the fracture strain is reduced with the increase of WC from 60.68 % to 44.46 %, this may be as a result of work-hardening, and consequently high strength (Nyanor et al., 2021).



**Fig. 6 Compression stress – strain curves of the  $(CrFeCoNi)_{1-x}(WC)_x$  ( $x=0-20$  wt.%) HEAs.**

As a result of enhancing the hardness and strength of the HEAs with the increase of WC content, an improvement in wear resistance of the HEAs is also expected due to Archard's wear equation (Eq. (1)) (R. Liu & Li, 2001) which states that the wear volume lose (V) is inversely proportional to the hardness (H) of the material and linearly proportional to the sliding distance (L) and normal load (F).

$$V = K \frac{LF}{H} \quad (1)$$

where (K) is a dimensionless constant known as the wear coefficient. This coefficient is a material constant which should be a function of other properties, such as the elasticity, surface quality, chemical affinity between the material of two surfaces and others.

Wear rate is the ratio of wear volume lose divided by normal load and total sliding distance, also the wear volume lose can be calculated by the wear area multiplied by the ball track distance. Fig. 7 demonstrates the results of wear rate of  $(\text{CrFeCoNi})_{1-x}(\text{WC})_x$  ( $x=0-20$  wt.%) HEAs as a function of WC percentage. It can be shown that the value of wear rate is gradually decreased with the increase of WC content. Also, the wear rate of  $(\text{CrFeCoNi})_{1.0}(\text{WC})_{0.0}$  HEA is  $(1.70\text{E}-04)$  which is approximately 4.5 times the wear rate of  $(\text{CrFeCoNi})_{0.8}(\text{WC})_{0.2}$  HEA ( $3.81\text{E}-05$ ), this means that wear resistance is significantly improved with the increase of WC content. This is also due to the dispersed WC phase in a homogeneous manner and the formed chromium carbide phases and the grain refinement. In which, addition of a hard ceramic material with a high strength and high thermal stability helps in the improvement of the wear resistance consequently the wear rate decreases and the life time of the fabricate tool is increased as the generated heat during any mechanical process. Work can not affect greatly on the sample performance due to the high dispersed WC thermal stability.

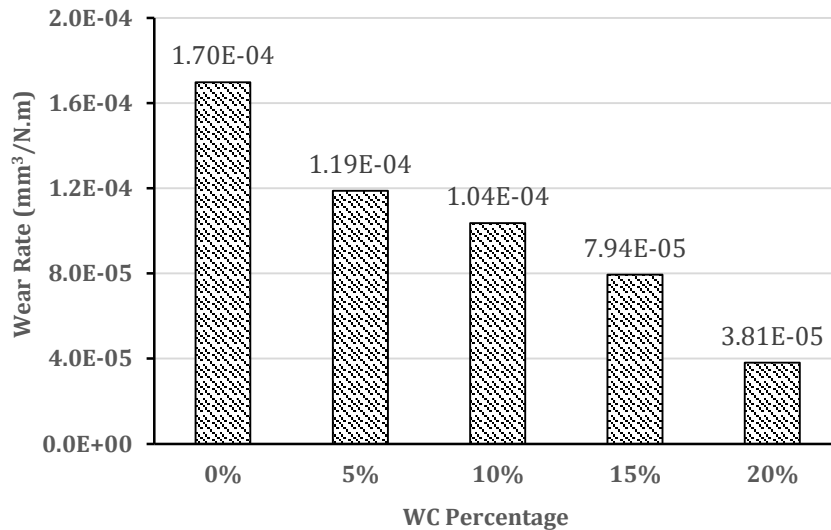


Fig. 7 Wear rate of the  $(\text{CrFeCoNi})_{1-x}(\text{WC})_x$  HEAs.

#### 4. Conclusions

1.  $(\text{CrFeCoNi})_{1-x}(\text{WC})_x$  HEAs were successfully prepared using PM technique. The relative density reached up to 97.0%, indicating the high sintering quality.
2. FCC HEA matrix phase, W-rich carbide, and two major types of Cr-rich carbides compose  $(\text{CrFeCoNi})_{1-x}(\text{WC})_x$  HEAs. Furthermore, W-rich carbide has a size of 5-10  $\mu\text{m}$ . The compositions of Cr rich carbides are complex, with fine Cr-rich phases in a size of sub-microns can be found.
3. The compressive strength is gradually increased with the increase of WC content. At the same time the fracture strain is approximately the same for all the specimens and it's exceeded 40%. This high compressive strength is owing to the good densification of the samples as a result of high relative density and low pore percentage.
4. The hardness of the  $(\text{CrFeCoNi})_{1-x}(\text{WC})_x$  HEAs steadily improved with increasing WC content, from 510.71 HV of the  $(\text{CrFeCoNi})_{1.0}(\text{WC})_{0.0}$  to 614.64 HV of the  $(\text{CrFeCoNi})_{0.80}(\text{WC})_{0.20}$ . The hard WC particle and the precipitation of Cr-rich carbides are most likely responsible for the strengthening mechanism.
5. The value of wear rate is gradually decreased with the increase of WC content. The wear rate of  $(\text{CrFeCoNi})_{1.0}(\text{WC})_{0.0}$  HEA is  $(1.70\text{E}-04)$  which is approximately 4.5 times higher than the wear rate of  $(\text{CrFeCoNi})_{0.8}(\text{WC})_{0.2}$  HEA ( $3.81\text{E}-05$ ), this means that wear resistance is significantly improved with the increase of WC content.

#### Acknowledgments

The authors acknowledge the financial and technical support from Central Metallurgical R&D Institute, and are greatly indebted for providing the materials used in this work, and introducing the microstructure facilities.

#### References:

1. Abu-Oqail, A., Wagih, A., Fathy, A., Elkady, O., & Kabeel, A. M. (2019). Effect of high energy ball milling on strengthening of Cu-ZrO<sub>2</sub> nanocomposites. *Ceramics International*, 45(5), 5866–5875. <https://doi.org/10.1016/j.ceramint.2018.12.053>
2. ASTM International. (2013). Standard Test Methods for Density of Compacted or Sintered Powder Metallurgy (PM) Products Using Archimedes' Principle. *Astm B962-15*, i, 1–7. <https://doi.org/10.1520/B0962-13.2>
3. Cantor, B., Chang, I. T. H., Knight, P., & Vincent, A. J. B. (2004). Microstructural development in equiatomic multicomponent alloys. *Materials Science and Engineering A*, 375–377(1-2 SPEC. ISS.), 213–218. <https://doi.org/10.1016/j.msea.2003.10.257>

4. Chuang, M. H., Tsai, M. H., Wang, W. R., Lin, S. J., & Yeh, J. W. (2011). Microstructure and wear behavior of Al<sub>x</sub>Co<sub>1.5</sub>CrFeNi<sub>1.5</sub>Ti<sub>y</sub> high-entropy alloys. *Acta Materialia*, 59(16), 6308–6317. <https://doi.org/10.1016/j.actamat.2011.06.041>
5. Coeffi, R. F. (2011). Standard Test Method for Linearly Reciprocating Ball-on-Flat Sliding Wear 1. *Lubrication*, 05(Reapproved 2010), 1–10. <https://doi.org/10.1520/G0133-05R10.2>
6. Dąbrowa, J., Cieślak, G., Stygar, M., Mroczka, K., Berent, K., Kulik, T., & Danielewski, M. (2017). Influence of Cu content on high temperature oxidation behavior of AlCoCrCuFeNi high entropy alloys (x = 0; 0.5; 1). *Intermetallics*, 84, 52–61. <https://doi.org/10.1016/j.intermet.2016.12.015>
7. Dong, Y., Zhou, K., Lu, Y., Gao, X., Wang, T., & Li, T. (2014). Effect of vanadium addition on the microstructure and properties of AlCoCrFeNi high entropy alloy. *Materials and Design*, 57, 67–72. <https://doi.org/10.1016/j.matdes.2013.12.048>
8. Elkady, O. A. M., Abu-Oqail, A., Ewais, E. M. M., & El-Sheikh, M. (2015). Physico-mechanical and tribological properties of Cu/h-BN nanocomposites synthesized by PM route. *Journal of Alloys and Compounds*, 625, 309–317. <https://doi.org/10.1016/j.jallcom.2014.10.171>
9. He, F., Wang, Z., Wu, Q., Li, J., Wang, J., & Liu, C. T. (2017). Phase separation of metastable CoCrFeNi high entropy alloy at intermediate temperatures. *Scripta Materialia*, 126, 15–19. <https://doi.org/10.1016/j.scriptamat.2016.08.008>
10. He, J. Y., Wang, H., Huang, H. L., Xu, X. D., Chen, M. W., Wu, Y., Liu, X. J., Nieh, T. G., An, K., & Lu, Z. P. (2016). A precipitation-hardened high-entropy alloy with outstanding tensile properties. *Acta Materialia*, 102, 187–196. <https://doi.org/10.1016/j.actamat.2015.08.076>
11. Hsu, C. Y., Sheu, T. S., Yeh, J. W., & Chen, S. K. (2010). Effect of iron content on wear behavior of AlCoCrFe<sub>x</sub>Mo<sub>0.5</sub>Ni high-entropy alloys. *Wear*, 268(5–6), 653–659. <https://doi.org/10.1016/j.wear.2009.10.013>
12. Huang, G., Hou, W., & Shen, Y. (2018). Evaluation of the microstructure and mechanical properties of WC particle reinforced aluminum matrix composites fabricated by friction stir processing. *Materials Characterization*, 138(January), 26–37. <https://doi.org/10.1016/j.matchar.2018.01.053>
13. Liu, B., Wang, J., Liu, Y., Fang, Q., Wu, Y., Chen, S., & Liu, C. T. (2016). Microstructure and mechanical properties of equimolar FeCoCrNi high entropy alloy prepared via powder extrusion. *Intermetallics*, 75, 25–30. <https://doi.org/10.1016/j.intermet.2016.05.006>
14. Liu, R., & Li, D. Y. (2001). Modification of Archard's equation by taking account of elastic/pseudoelastic properties of materials. *Wear*, 250–251(PART 2), 956–964. [https://doi.org/10.1016/s0043-1648\(01\)00711-6](https://doi.org/10.1016/s0043-1648(01)00711-6)
15. Löbel, M., Lindner, T., Mehner, T., & Lampke, T. (2018). Influence of titanium on microstructure, phase formation and wear behaviour of AlCoCrFeNiTi<sub>x</sub> high-entropy alloy. *Entropy*, 20(7), 1–11. <https://doi.org/10.3390/e20070505>
16. Luo, W., Liu, Y., Luo, Y., & Wu, M. (2018). Fabrication and characterization of WC-AlCoCrCuFeNi high-entropy alloy composites by spark plasma sintering. *Journal of Alloys and Compounds*, 754, 163–170. <https://doi.org/10.1016/j.jallcom.2018.04.270>
17. Luo, W., Liu, Y., & Tu, C. (2021). Wetting behaviors and interfacial characteristics of molten Al<sub>x</sub>CoCrCuFeNi high-entropy alloys on a WC substrate. *Journal of Materials Science and Technology*, 78, 192–201. <https://doi.org/10.1016/j.jmst.2020.10.067>
18. Nyanor, P., El-Kady, O., Yehia, H. M., Hamada, A. S., & Hassan, M. A. (2021). Effect of Bimodal-Sized Hybrid TiC–CNT Reinforcement on the Mechanical Properties and Coefficient of Thermal Expansion of Aluminium Matrix Composites. *Metals and Materials International*, 27(4), 753–766. <https://doi.org/10.1007/s12540-020-00802-w>
19. Poletti, M. G., Fiore, G., Gili, F., Mangherini, D., & Battezzati, L. (2017). Development of a new high entropy alloy for wear resistance: FeCoCrNiW<sub>0.3</sub> and FeCoCrNiW<sub>0.3</sub> + 5 at.% of C. *Materials and Design*, 115, 247–254. <https://doi.org/10.1016/j.matdes.2016.11.027>
20. Sadoun, A. M., Mohammed, M. M., Elsayed, E. M., Meselhy, A. F., & El-Kady, O. A. (2020). Effect of nano Al<sub>2</sub>O<sub>3</sub> coated Ag addition on the corrosion resistance and electrochemical behavior of Cu–Al<sub>2</sub>O<sub>3</sub> nanocomposites. *Journal of Materials Research and Technology*, 9(3), 4485–4493. <https://doi.org/10.1016/j.jmrt.2020.02.076>
21. Sadoun, A. M., Mohammed, M. M., Fathy, A., & El-Kady, O. A. (2020). Effect of Al<sub>2</sub>O<sub>3</sub> addition on hardness and wear behavior of Cu–Al<sub>2</sub>O<sub>3</sub> electro-less coated Ag nanocomposite. *Journal of Materials Research and Technology*, x x. <https://doi.org/10.1016/j.jmrt.2020.03.020>
22. Shang, C., Axinte, E., Ge, W., Zhang, Z., & Wang, Y. (2017). High-entropy alloy coatings with excellent mechanical, corrosion resistance and magnetic properties prepared by mechanical alloying and hot pressing sintering. *Surfaces and Interfaces*, 9(June), 36–43. <https://doi.org/10.1016/j.surfin.2017.06.012>
23. Shang, C., Axinte, E., Sun, J., Li, X., Li, P., Du, J., Qiao, P., & Wang, Y. (2017). CoCrFeNi(W<sub>1</sub> – xMox) high-entropy alloy coatings with excellent mechanical properties and corrosion resistance prepared by mechanical alloying and hot pressing sintering. *Materials and Design*, 117, 193–202. <https://doi.org/10.1016/j.matdes.2016.12.076>
24. Stepanov, N. D., Yurchenko, N. Y., Tikhonovsky, M. A., & Salishev, G. A. (2016). Effect of carbon content and annealing on structure and hardness of the CoCrFeNiMn-based high entropy alloys. *Journal of Alloys and Compounds*, 687, 59–71. <https://doi.org/10.1016/j.jallcom.2016.06.103>
25. Tang, Z., Yuan, T., Tsai, C. W., Yeh, J. W., Lundin, C. D., & Liaw, P. K. (2015). Fatigue behavior of a wrought Al<sub>0.5</sub>CoCrCuFeNi two-phase high-entropy alloy. *Acta Materialia*, 99, 247–258. <https://doi.org/10.1016/j.actamat.2015.07.004>
26. Torralba, J. M., & Venkatesh Kumarán, S. (2021). Development of competitive high-entropy alloys using commodity powders. *Materials Letters*, 301(June), 130202. <https://doi.org/10.1016/j.matlet.2021.130202>
27. Tsai, M. H., Fan, A. C., & Wang, H. A. (2017). Effect of atomic size difference on the type of major intermetallic phase in

- arc-melted CoCrFeNiX high-entropy alloys. *Journal of Alloys and Compounds*, 695, 1479–1487. <https://doi.org/10.1016/j.jallcom.2016.10.286>
28. Tung, C. C., Yeh, J. W., Shun, T. tsung, Chen, S. K., Huang, Y. S., & Chen, H. C. (2007). On the elemental effect of AlCoCrCuFeNi high-entropy alloy system. *Materials Letters*, 61(1), 1–5. <https://doi.org/10.1016/j.matlet.2006.03.140>
  29. Xu, J., Wang, S., Shang, C., Huang, S., & Wang, Y. (2019). Microstructure and properties of CoCrFeNi(WC) high-entropy alloy coatings prepared using mechanical alloying and hot pressing sintering. *Coatings*, 9(1). <https://doi.org/10.3390/coatings9010016>
  30. Yeh, J. (2013). Alloy Design Strategies and Future Trends in High-Entropy Alloys. *The Minerals, Metals & Materials Society Alloy*, 65(12), 1759–1771. <https://doi.org/10.1007/s11837-013-0761-6>
  31. Yehia, H. M., El-Tantawy, A., Ghayad, I. M., Eldesoky, A. S., & El-kady, O. (2020). Effect of zirconia content and sintering temperature on the density, microstructure, corrosion, and biocompatibility of the Ti–12Mo matrix for dental applications. *Journal of Materials Research and Technology*, 9(4), 8820–8833. <https://doi.org/10.1016/j.jmrt.2020.05.109>
  32. Yilbas, B. S., Toor, I. U. H., Malik, J., & Patel, F. (2014). Laser gas assisted treatment of AISI H12 tool steel and corrosion properties. *Optics and Lasers in Engineering*, 54, 8–13. <https://doi.org/10.1016/j.optlaseng.2013.10.004>
  33. Zhou, R., Chen, G., Liu, B., Wang, J., Han, L., & Liu, Y. (2018). Microstructures and wear behaviour of (FeCoCrNi)<sub>1-x</sub>(WC)<sub>x</sub> high entropy alloy composites. *International Journal of Refractory Metals and Hard Materials*, 75(November 2017), 56–62. <https://doi.org/10.1016/j.ijrmhm.2018.03.019>